Small-Scale Rain Nonuniformity and Its Effect on Evaluation of Nonuniform Beam-Filling Error for Spaceborne Radar Rain Measurement

LING ZHANG, DAREN LU, SHU DUAN, AND JINLI LIU

LAGEO, Institute of Atmospheric Physics, Chinese Academy of Sciences, Beijing, China

(Manuscript received 21 March 2003, in final form 23 February 2004)

ABSTRACT

An observational method has been proposed to sample radar echo with high range resolutions using a ground-based meteorological radar. Utilizing this method, the rainfall echo data with a high range resolution of 125 m was obtained by using an X-band meteorological radar. The analysis of rain nonuniformity strength using these high-resolution radar data shows that the nonuniformity is significant and, even in an instantaneous field of view (IFOV) of 1 km, the reflectivity excursion above 10 dB is common. The simulation of the nonuniform beam filling (NUBF) error of the path-integrated attenuation (PIA) measured by the spaceborne radar has been also implemented using these data. The results show that the PIA encounters mainly underestimation and cannot be neglected; even in 0.5-km IFOV the underestimation can reach up to 50%. The correlation analyses show that the relative PIA error and the standard deviation of rain rate have a power-law relationship with quite good correlation, which might be used to partially correct this error. The simulation also shows that it is very important to use the high-resolution data in studying the NUBF error of the next-generation spaceborne radar with a higher across-beam resolution (e.g., below 3 km).

1. Introduction

It is well known that nonuniform rain filling within radar resolution volume causes a spatial smoothing error for quantitative radar rainfall measurement because of nonlinear relationships between radar observables and rain rate. Especially, such smoothing error becomes more significant for a spaceborne radar whose resolution size is comparable to or larger than a convective rain cell size. The smoothing error is usually studied in the two cross radar beam dimensions because it is much more difficult to deal with the nonuniformity across the beam than that along the beam, thus nonuniform filling in the resolution volume becomes what is commonly referred to as nonuniform beam filling (NUBF; Testud et al. 1992, 1996; Amayenc et al. 1993, 1996; Durden et al. 1998; Kozu and Iguchi 1999). Analyses of the smoothing error due to NUBF have found biases in retrieved rain rate for a spaceborne radar. Biases in the spaceborne radar–retrieved rain rate due to NUBF have been analyzed by a number of authors using a nonuniform rain cell model, rain gauge data, or ground-based radar data (Nakamura 1991; Testud et al. 1992, 1996; Amayenc et al. 1993). Amayenc et al. (1996) studied the bias due to NUBF using nadir-looking airborne radar data for a rainstorm near Wallops Island, Virginia. Durden et al. (1998) also studied the NUBF bias using data from the Airborne Rain Mapping Radar (ARMAR) for precipitation in the western Pacific Ocean during the Tropical Ocean and Global Atmosphere Coupled Ocean–Atmosphere Response Experiment (TOGA COARE). The ARMAR is a simulator of the spaceborne precipitation radar (PR) of the Tropical Rainfall Measuring Mission (TRMM). In order to enhance radar resolution, Zhang et al. (1998) proposed a deconvolution method for retrieving nonuniform reflectivities in the radar beam and tested the method using artificial sinusoidal variation reflectivities and ground-based radar observation data. Kozu and Iguchi (1999) put forward a method for correcting the NUBF bias and appraised the method using shipborne radar data during the TOGA COARE.

There have been a number of works mentioned above concerning NUBF in which parameterization models, rain gauge data, or radar data were used to describe rain structures, but the resolution of radar data, which is the best way to represent the real rain structure, was primarily around 1 km or more in the aforementioned works. The 1-km-resolution radar data might smooth out variations within small scales less than 1 km and result in the error in the smoothing error analysis. How much is the nonuniformity of the rainfall field within less than 1-km spatial scale and its influence on the radar rainfall measurement smoothing? In order to investigate

Corresponding author address: Ling Zhang, LAGEO, Institute of Atmospheric Physics, Chinese Academy of Sciences, Beijing 100029, China.
E-mail: lzhang@mail.iap.ac.cn

TABLE 1. The main specifications of the X-band radar.

Parameter	Value
Antenna aperture (diameter)	1.25 m
Beamwidth (−3 dB)	1.8°
Antenna gain	37 dB
Frequency	9375 MHz
Peak power	200 kW
Pulse duration	0.6 μs
Pulse repetition frequency	1500 Hz
Noise figure	3.6 dB
Bandwidth	1.5 MHz
Minimum detectable reflectivity	−8 dB*Z* (at 10 km)

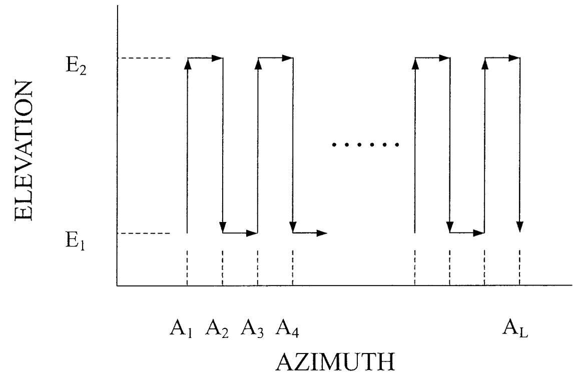

FIG. 1. Track of vertical antenna scan in an azimuth sector.

this problem, we implemented rain observations with a high range resolution of 125 m using a 3-cm-wavelength meteorological radar in the summer of 2000 at a site (39°45′N, 116°58′E) near Beijing, and then used this high-resolution radar dataset to simulate the spatial smoothing error of the *Z–R* relationship based radar rainfall measurement (Zhang et al. 2003). We found that the small-scale rain nonuniformity is significant, and, even in a spatial smoothing window of 1-km size, it is significant. Computations indicated that owing to the significant rain nonuniformity, the rain-rate smoothing error cannot be neglected, and even for a smoothing window of 0.5-km size, similar to resolutions of ground-based radars, the error can be above 30%. Comparisons of the smoothing errors computed from radar data between the 125-m high resolution and the 1-km low resolution showed that the smoothing errors from the 1-km-resolution data would be underestimated. The underestimation would be about 25% for smoothing windows of 4 and 3 km and about 40% for that of 2 km. In order to find possible good correlations between the smoothing error and other parameters, correlation analysis between the smoothing error and average reflectivity, strength of nonuniformity, true rain rate, and size of radar resolution volume were also analyzed in that paper. We found an encouraging good correlation that the relative smoothing error and the maximum excursion (defined as the reflectivity difference between maximum and minimum) has a quite good power relation whose correlation coefficient exceeds 0.9, which might be used in the radar signal processing to correct the nonuniformity error.

In this work, following the work of Zhang et al. (2003), we investigate the statistical nature of the spatial smoothing error due to NUBF in the spaceborne radar rain measurement based on a surface reference technique (SRT) using the high-resolution radar data. We begin by giving a description of the high-resolution rain observation of radar and its acquired data. Following this we describe the smoothing error simulation algorithm. The simulation results using the obtained radar data are then presented.

2. High-resolution rain observation

The deployed radar for our rain observations is an X-band meteorological radar whose main technical specifications are listed in Table 1. The resolution of reflectivity data obtained in the operational observation of a conventional ground-based meteorological radar is typically 1 km. Therefore, under the condition that radar scheme, specifications, and acquired reflectivity accuracy are all to be unmodified if we want to enhance the radar measurement resolution to less than 1 km, we can only decrease the integrating times along range by increasing the integrating times across range, lowering scanning speed, and reducing the spatial coverage of observations. Based on this concept, we designed a special radar scan mode, given in Fig. 1, to carry out the high-resolution measurements. As pictured in Fig. 1, the antenna scan rate is slowed down and scans vertically within a range of elevation (from E_1 to E_2) at several adjacent azimuths ($A_1, A_2, \ldots, A_L$) with an identical interval in an azimuth sector (between A_1 and A_L). The radar scanning begins at (A_1, E_1), subsequently following the path in Fig. 1 goes to (A_1, E_2), (A_2, E_2), (A_2, E_1), . . . , and (A_L, E_1) consecutively, completes one cycle, then restarts at (A_1, E_1) and begins a next cycle, finally ending when a specified number of cycles are all covered. In this vertical solid sector scan, the radar samples rain echoes with a high range resolution of 125 m. To implement the high-resolution observation, the extent of elevation (E_1 and E_2) and azimuth (A_1 and A_L) is chosen from the real-time distribution of rain echoes on conventional PPI display at a normal scanning speed first, and the number of azimuths (L) and the azimuth interval are then chosen according to A_1 and A_L.

During the three rainfall processes on 22 August and 4 and 20 September 2000 near Beijing, we obtained a large quantity of rain echo data with a range resolution of 125 m from the X-band radar working in a vertical solid sector scan mode. These data have been used to simulate the smoothing error of spaceborne radar rain measurement in this paper.

3. Simulation algorithm

This paper focuses on rain nonuniformity at small scales less than 1 km and its effects on NUBF error of spaceborne radar rain measurement, and does not involve an elaborate rain model or an elaborate rain retrieval algorithm, thus a relative simple rain model and a simple rain retrieval algorithm are assumed in the NUBF error simulation. Although the assumed model and algorithm are simple, they should reveal the primary characteristics of the NUBF error. In our high-resolution radar observation mode, the range resolution is controlled by the signal processing and set to 125 m, whereas the cross-range resolution is determined by range and radar beamwidth. The cross-range resolution of radar is formulated as θr, where r is the range of rain target offset to radar, and θ is the radar beamwidth. Using the specifications in Table 1 to calculate the cross-range resolution, one can obtain the resolution of 0.3 km at a range of 10 km and 1.6 km at 50 km. The resolution of radar data in this work is high along beam with the fixed value of 125 m but across beam is lower, variable, and gets worse as the range increases; therefore, only one-dimensional integration is considered in our smoothing error simulations.

In rain-rate retrieval from spaceborne radar, the path-integrated attenuation (PIA), which can be obtained by the SRT, is a very important parameter since it provides a constraint to stabilize the rain attenuation correction procedure for retrieving heavy rain rate and, in addition, it can be directly converted to path-integrated rain rate due to the approximately linear relationship between attenuation and rain rate (Meneghini et al. 1983; Amayenc et al. 1993; Testud et al. 1996; Durden et al. 1998; Iguchi and Meneghini 1994; Iguchi et al. 2000). Therefore, it has become a crucial task to understand the NUBF influences on the PIA and, if possible, to develop an algorithm to correct for them. In this work only the NUBF error of the PIA is chosen for study.

According to the above reasons, we used a simulation technique similar to that used by Kozu and Iguchi (1999) but simpler. This technique is described in the following. A rain cell model illuminated in an instantaneous field of view (IFOV) by a spaceborne radar is assumed. This rain cell model, illustrated in Fig. 2, is vertically uniform and horizontally nonuniform, with a depth of 5 km. In order to be consistent with the high-resolution radar data in horizontal plane, the rain cell is assumed to be nonuniform in only one dimension corresponding to the along-range variation of radar reflectivities but uniform in the other dimension. The IFOV is assumed to be square shaped for simplicity and with a side length of Δr_m, that is, the resolution of the spaceborne radar. If the reflectivity factor, the rain rate, and the specific attenuation of rain for the ith rain element in the IFOV are represented by Z_{hi}, R_{hi}, and k_{hi}, respectively, the power law Z–R and k–R relationship can be written

$$Z_{hi} = aR_{hi}^b, \qquad k_{hi} = cR_{hi}^d, \tag{1}$$

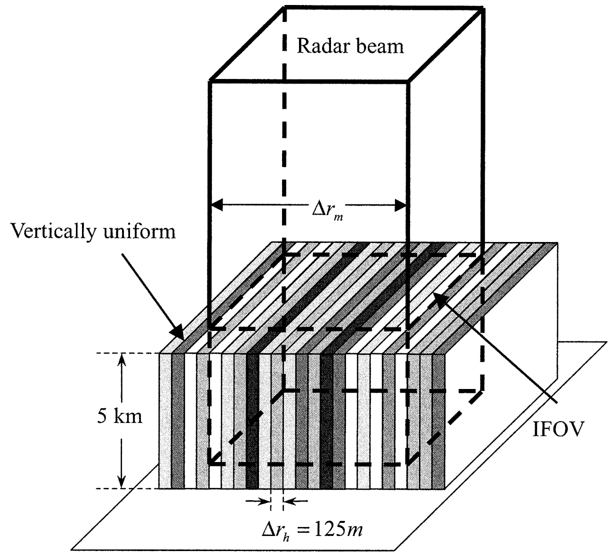

FIG. 2. Schematic diagram of rain cell sensing by a spaceborne radar.

where Z_{hi} is in mm^6 m^{-3}, R is in mm h^{-1}, a and b are constants, k is in dB km^{-1}, a and c are constant coefficients with b and d exponents. In using the Z–R relationship, it is better to choose appropriate values of the constant a and b that are derived from raindrop size distribution (DSD), which is closer to that in a real rainfall processes. Since the radar data are obtained near Beijing and the rain rate R is calculated direct from reflectivity factor Z, we utilize the empirical Z–R relationships derived from the real raindrop size distributions observed in China by the Institute of Atmospheric Physics, affiliated with the Chinese Academy of Sciences, and choose the values for Beijing district at 3-cm wavelength (Microwave Remote Sensing Group 1982, p. 127). These values are $a = 236.8$ and $b = 1.569$. Here it is the spaceborne radar for which we simulate the rain NUBF error; hence, we choose the values of c and d derived from Marshall–Palmer DSD (Marshall and Palmer 1948) at 13.8 GHz of the TRMM PR spaceborne radar in the work done by Marecal et al. (1997). Their computed values are $c = 0.0230$ and $d = 1.190$.

Given the specific attenuation k_{hi} in the IFOV, the radar measured two-way PIA from the SRT, A_{sm}, in decibels, can be computed by averaging over the IFOV:

$$A_{sm} = -10 \lg\left[\frac{1}{N}\sum_{i=1}^{N} \exp\left(-\frac{\ln 10}{10}k_{hi} \times 2H\right)\right],$$
$$N = \frac{\Delta r_m}{\Delta r_h}, \tag{2}$$

where the subscript s and m denote the ‘‘SRT’’ and the ‘‘measured,’’ respectively; N is the number of rain elements within the IFOV; H is the rain cell depth and is 5 km; and Δr_h is the range resolution of the high-resolution radar data and equals 0.125 km. Here we make use of the uniform PIA, A_u, which is defined as the PIA converted from average rain rate with a k–R relationship when rain is assumed uniform in the IFOV:

$$A_u = 2Hc\left(\frac{1}{N}\sum_{i=1}^{N} R_{hi}\right)^d. \quad (3)$$

Because of the nonuniformity of rain in the IFOV and the high nonlinearity of the relationship between attenuation and rain rate, the measured PIA A_{sm} and the uniform PIA A_u are different, and it is also impossible to derive the A_u from the radar measurement A_{sm}. The difference between the measured value A_{sm} and the uniform value A_u is the spatial smoothing error due to the NUBF, as referred to in this paper. Here the spatial smoothing means that the spatially nonuniform rain is smoothed by the averaging effects of the spaceborne radar antenna IFOV. Let the absolute and the relative PIA error due to the NUBF be denoted by ΔA and δA, respectively, and can be formulated as

$$\Delta A = A_{sm} - A_u, \qquad \delta A = \frac{\Delta A}{A_u}. \quad (4)$$

Here the PIA error is not a real error of PIA measurement from spaceborne radar; it is just a form of address for convenience and represents the NUBF effects. In order to quantitatively express the strength of rain nonuniformity, a parameter defined as the difference between the maximum and minimum of reflectivities in the IFOV, named as the reflectivity excursion, is introduced. It is only for simplicity that this parameter is used, although there might be other parameters to describe the nonuniformity, such as the standard deviation. If the reflectivity excursion is symbolized by DZ, it can be written as

$$\mathrm{DZ} = \max_{i=1,\ldots,N}(10 \times \log Z_{hi}) - \min_{i=1,\ldots,N}(10 \times \log Z_{hi}). \quad (5)$$

Using the reflectivity factors of the high-resolution radar data as the inputs of Z_{hi} and computing Eqs. (1)–(5), the uniform PIA A_u, the NUBF error ΔA and δA, and the nonuniformity strength DZ, etc., can be all calculated.

4. Results

a. Data processing and computation

Before the simulation was carried out, some constraints were set for the selection of the radar data that would be used in the NUBF error simulation. The range of radar ray elevation angles is chosen from 3° to 20° above the horizon so that the chosen radar rays are high enough to avoid touching any surface targets or ground clutter and to meet only precipitating cloud particles, and also are not too high to represent horizontal nonuniformities of rainfall. The minimum reflectivity is set to 18 dB*Z* in the simulation to guarantee that the reflectivities used in the simulation are substantially beyond the radar noise level at all range bins, because the radar minimum detectable reflectivity is between −28 and 12 dB*Z* for ranges from 1 to 100 km.

Since the data are from an X-band radar, which suffers attenuation in heavy rain, it needs to be corrected for attenuation. The radar data were processed for attenuation correction using the H–B solution given by Hitschfeld and Bordan (1954) A k–R relationship for the Beijing district at 3-cm wavelength (Microwave Remote Sensing Group 1982, p. 127) is chosen and used in the H–B solution. The constant coefficient and the exponent of this k–R relationship are $c = 0.0112$ and $d = 1.202$. Since the H–B solution can be unstable at high rain rates, we need to perform a quality control evaluation of the data that has undergone the attenuation correction. In order to make use of reliable data, we determined a criterion based on our experience from the attenuation correction process. The criterion is that, if the two-way PIA in a radar ray is greater than 30 dB, the corrected reflectivity data in this ray are suspected to be unreliable and are excluded in the simulation.

For each of the chosen radar rays, all range bins are divided into a number of segments and each of the segments has a sum of N range bins. The reflectivities in every segment have a number of N values and can be used to obtain one value for the parameters in one spaceborne radar IFOV described in section 3. In order to delete suspected unreliable big values, we determined a maximum limit of 60 dB*Z*. If there is any attenuation-corrected reflectivity greater than 60 dB*Z* in an IFOV, this IFOV will be excluded in the simulation. The reflectivity data for every radar ray that satisfies the above constraints are all taken for the simulation.

In the simulation of the NUBF error, the sizes of the IFOV were chosen as 0.5, 1, 2, 3, and 4 km; that is, $\Delta r_m = 0.5$, 1, 2, 3, and 4 km. In addition to the NUBF error, several other parameters, such as the nonuniformity strength, the uniform PIA, the averaged reflectivity, etc., were computed according to the equations in section 3. The possible correlations between these parameters were also analyzed. The simulation results will be given in the following subsections.

b. Nonuniformity strength of rain

In order to understand how much the rain nonuniformity in the IFOV is, the reflectivity excursion DZ and the averaged reflectivity, that is, the average of high-resolution reflectivity Z_{hi} in the IFOV, were computed using the 125-m range resolution radar data obtained from the three rainfall processes, and the scatterplots for the DZ and the averaged reflectivity were also made. One scatterplot obtained from the rainfall process on 22 August 2000 is given in Fig. 3.

Figure 3 indicates that the rain nonuniformity is serious. It can be seen that the reflectivity excursion scatters extensively from near 0 to around 35 dB, and even

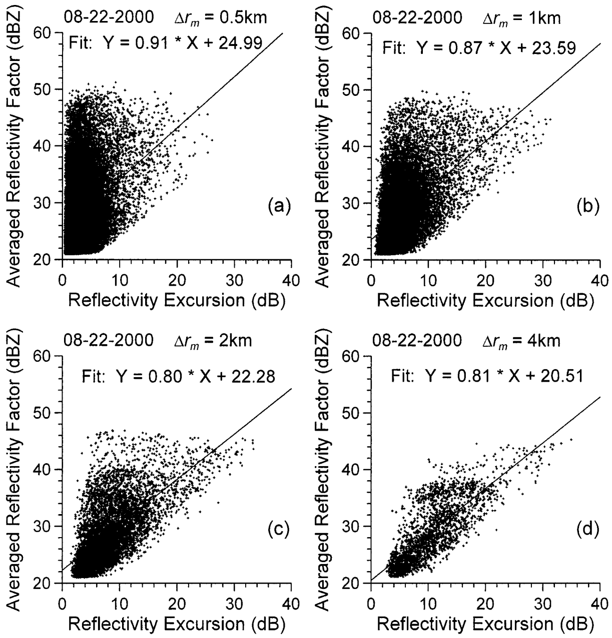

FIG. 3. Scatterplot of the averaged reflectivity factor vs the reflectivity excursion obtained from the rain observations on 22 August 2000. The straight line is a linear fit with its equation given. The IFOV sizes are (a) 0.5, (b) 1, (c) 2, and (d) 4 km.

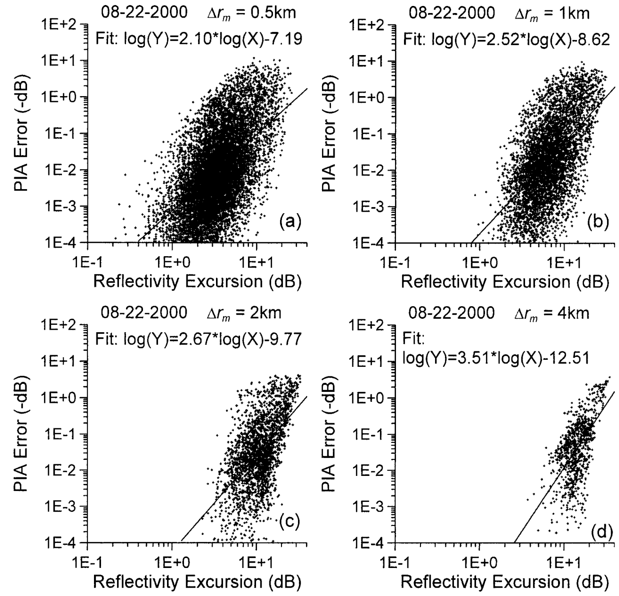

FIG. 4. Scatterplot of the PIA NUBF error vs the reflectivity excursion obtained from the same rain data as in Fig. 3. The straight line is a power fit with its equation given. The IFOV sizes are the same as in Fig. 3.

within the IFOV of 1-km size [in Fig. 3b], it can reach over 10 dB. The reflectivity excursion increases when the IFOV size increases from 0.5 km [in Fig. 3a] to 4 km [Fig. 3d]. In Fig. 3a, the minimum reflectivity excursion within 0.5 km is about 0 dB; that is, the rain is uniform within the IFOV. The reason that the minimum reflectivity in Fig. 3a is not exactly zero is that the values of the excursion below 0.4 dB were not plotted in order to avoid the points on the vertical axis and to see the axis clearly. In the computations, averaged reflectivities below 21 dB*Z* (i.e., 3 dB above the minimum reflectivity limit 18 dB*Z*) were not output in order to avoid the influence of this limit, so the reflectivities below 21 dB*Z* cannot be seen. From Figs. 3a–d, the minimum excursion increases from 0 to about 3 dB as the IFOV size increases from 0.5 to 4 km. Although the correlation between the excursion and the averaged reflectivity is low and that this is consistent with the considerable difficulty for correcting the NUBF error, it can be seen that the reflectivity excursion tends to increase as the averaged reflectivity increases in the statistical sense from the linear fits shown in this figure. The computations for the radar data of the other two rain processes also indicated the similar results reasonably consistent with those in Fig. 3.

c. PIA NUBF error versus reflectivity excursion

The NUBF error is caused by the rain nonuniformity in the IFOV; therefore, it should have some correlation with the rain nonuniformity strength. In order to understand the correlation between them, we computed the PIA error ΔA and the reflecitivity excursion DZ for the radar data of the three rainfall processes. One scatterplot of ΔA versus DZ obtained from the data of the rainfall process, identical to the process in Fig. 3, is given in Fig. 4.

Our computations indicated that the SRT-based spaceborne radar PIA estimate would mainly be underestimated because of the rainfall nonuniformity and the nonlinear relationship between the PIA and the rain rate, which agrees with the findings of other authors (Nakamura 1991; Amayenc et al. 1993, 1996; Testud et al. 1996; Durden et al. 1998; Kozu and Iguchi 1999). At the same time, our computations also indicated that the PIA would suffer very little overestimation when the rain rate is small. We will explain this phenomenon in a later subsection. This overestimation is not seen in Fig. 4 because values below zero cannot be plotted on the logarithmic scale axis.

It can be seen in Fig. 4 that the PIA error varies largely from near 0 to about 10 dB and has a very low correlation with the reflectivity excursion. Nevertheless, the PIA error increases with increasing reflectivity excursion in the statistical sense as the linearly logarithmic fits show in Fig. 4. The slope of the linear fit line in dual-logarithm scale increases a bit, but the intercept also decreases with increasing IFOV size. However, our calculations of the average PIA error indicated that, in the statistical sense, as the IFOV size increases, the reflectivity excursion increases, and this results in that the PIA error increases too.

In order to search for possible better correlations be-

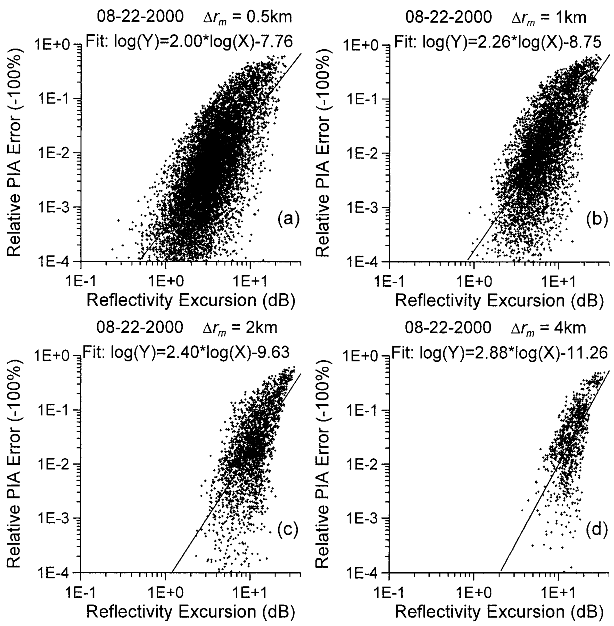

FIG. 5. As in Fig. 4 except for the relative PIA NUBF error vs the reflectivity excursion.

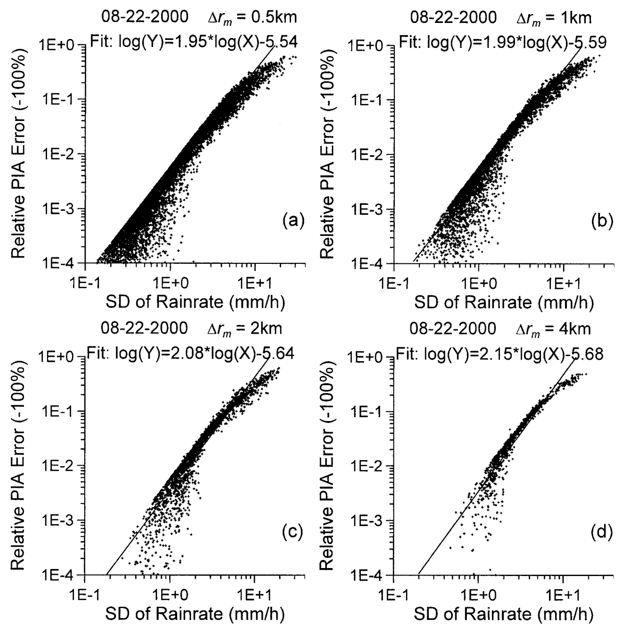

FIG. 6. As in Fig. 4 except for the relative PIA NUBF error vs the SD of rain rate.

tween the NUBF error and the reflectivity excursion, we computed the relative PIA error δA. One scatterplot of δA versus DZ obtained from the radar data identical to that in Fig. 4 is shown in Fig. 5. It can be seen in Fig. 5 that the relative PIA error disperses from near 0% to about 50% and also has low correlation with the reflectivity excursion, but in the statistical sense it increases with the increasing of the reflectivity excursion. The relationship between the relative PIA error and the reflectivity excursion is similar to that between the PIA error and the reflectivity excursion. This feature is different from that for the *Z–R* relationship-based relative rain-rate error, where the relative rain-rate smoothing error and the reflectivity excursion have a good correlation (the correlation coefficient is higher than 0.9) and display a power-law relationship (Zhang et al. 2003). It also can be seen in Fig. 5 that, even for the IFOV size of 0.5 km similar to that of a ground-based radar, the relative PIA error can reach up to 50%, though it is highly spread for each of the other larger IFOV sizes. Therefore, the NUBF error must not be neglected, and it is very important to find a possible method for correcting it.

d. PIA NUBF error versus other parameters

In order to look for possible correlations between the NUBF error and other parameters continuously, we analyzed the correlations of the PIA error versus the uniform PIA, the relative error versus the uniform PIA, the PIA error versus the standard deviation (SD) of rain rate, the relative error versus the SD of rain rate, the PIA error versus the normalized standard deviation (NSD) of rain rate, and the relative error versus the NSD of rain rate. We found a relatively better correlation between the relative error and the SD of rain rate. For the radar data of the rainfall that occurred on 22 August 2000, the scatterplot of the relative error versus the SD of rain rate is given in Fig. 6. It can be seen in Fig. 6 that the relative error and the SD of rain rate have a quite good correlation to some extent and exhibit a power-law relationship. The calculations using the data observed for the other two rainfall events on 4 and 20 September 2000 also gave a power-law relationship that reasonably agrees with that in Fig. 6.

Although the PIA NUBF error spreads extensively, an encouraging correlation was found in our simulation that the relative NUBF error has a power-law dependence on the SD of rain rate. This power-law dependence might be used in the rain retrieval algorithm for partially correcting the NUBF error.

As we showed in sections 4b and 4c, in the statistical sense, when the intensity of rain increases, the rain nonuniformity very likely increases; at the same time the PIA NUBF error and the relative PIA NUBF error very likely increase as well. This implies that the NUBF error correction is more significant for large rain rates, relative to small rain rates. However, how to make the NUBF error correction to achieve optimal results in practice is beyond the scope of this paper, and will be left to future work.

e. NUBF error simulation with high- and low-resolution data

Some works have been done to study the NUBF error of spaceborne radar rain measurements by several au-

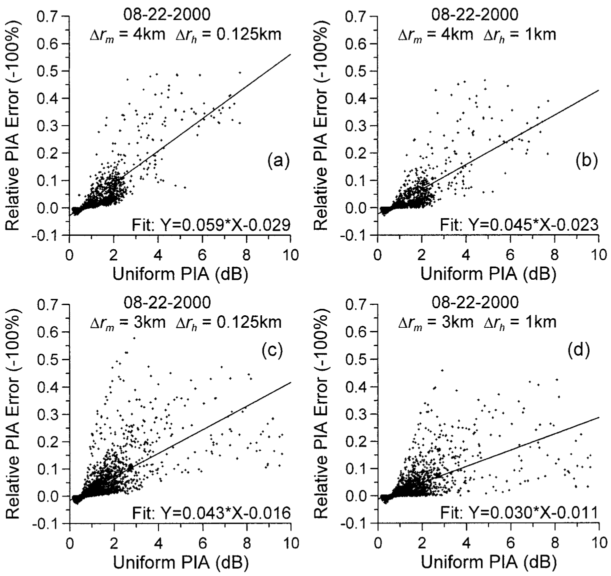

FIG. 7. Scatterplot of the relative PIA NUBF error vs the uniform PIA obtained from the same rain data as those in Fig. 3. The straight line is a linear fit with its equation given. The IFOV sizes are (a) 4, (b) 4, (c) 3, and (d) 3 km. The resolutions of data used are (a) 0.125 (high), (b) 1 (low), (c) 0.125, and (d) 1 km.

thors. However, in their works, the resolution of all the radar data that they utilized were about 1 km or more. These low-resolution data would cause errors in the NUBF error simulation because the real rain cell has nonuniformity within small scales less than 1 km, as we indicated in section 4b. Therefore, it is important to know the magnitude of error due to using lower-resolution radar data. In order to deal with this question, we compared results between the 125-m-resolution data and the 1-km-resolution data. Before the NUBF simulation was done, the 1-km-resolution dataset was obtained by averaging the 125-m-resolution data over every 8-range-bin segment. Then the simulation was made by using the 125-m-resolution data and the 1-km-resolution data, respectively. An example of scatterplots of the relative PIA error versus the uniform PIA obtained in the same rainfall process as that of Fig. 3 is given in Fig. 7. In Fig. 7, the results are in the left column [Fig. 7a, c] for the 125-m resolution and on the right column [Fig. 7b, c] for the 1-km resolution.

It can be seen in Fig. 7 that, when the PIA is below about 1 dB, the PIA is overestimated, usually below 5%, corresponding to the possible biggest value of 0.05 dB, which can be neglected. We can explain this overestimation as follows. When the PIA is small, the rain rate and the specific attenuation are also small, and Eq. (2) can be simplified by approximation. From Eqs. (2) and (1), we can derive

$$A_{sm} \approx \frac{1}{N}\sum_{i=1}^{N} gR_{hi}^{d}, \qquad g = 2Hc, \tag{6}$$

by making use of the two mathematical approximate equations,

$$e^{x} \approx 1 + x, \qquad \ln(1 + x) \approx x,$$
$$(\text{when } |x| \text{ is small}). \tag{7}$$

We can see in Eq. (6) that the measured PIA is the mean of a power function

$$F(R) = gR^{d}, \qquad (d > 1). \tag{8}$$

In mathematics, there is a following law for this power function, whose second derivative is always positive:

$$\overline{F(R)} > F(\overline{R}), \tag{9}$$

where the bars over the variables denote average. Equation (9) accounts for the fact that the measured PIA is greater than the uniform PIA (i.e., overestimation) when the PIA is small enough.

Comparing Figs. 7a and 7c to Figs. 7b and 7d, the slopes of linear fit lines are lower in the right column than those in the left; this means that using low- (1-km) resolution data brings forth error underestimation in the NUBF error simulation in the statistical sense. The slope of fit is lower by 24% in Fig. 7b than that in Fig. 7a, and lower by 30% in Fig. 7d than that in Fig. 7c, which implies that, in the statistical sense, using the low-resolution data causes error underestimation with 24% for the 4-km IFOV and 30% for the 3-km IFOV. Comparison for the IFOV size of 2 km indicated that using the low (1 km) resolution data would result in error underestimation with 52%. (The scatterplot for the 2-km IFOV size is not given in Fig. 7.)

From the above statistical analysis, it can be concluded that the difference of the NUBF error estimations between using the 125-m-resolution data and using the 1-km-resolution data is evident and not neglectable, and also increases with the decreasing of the IFOV size.

5. Conclusions

We have proposed an observational method for a ground-based meteorological radar to acquire high range resolution reflectivities of echoes returned from precipitating clouds. Using this method, we made observations of the fine structures of rainfall in the summer of 2000 near Beijing with an X-band meteorological radar. We obtained the reflectivity data with a high range resolution of 125 m in three rainfall events during these observations. Then we used these data to compute the nonuniformity strength expressed by the reflectivity excursion in decibels, the averaged reflectivity, the uniform PIA, the SD of rain rate in the IFOV, and to simulate the nonuniform beam-filling error of the PIA by the surface reference technique in spaceborne radar.

The computations of the nonuniformity strength indicated that the nonuniformity is significant and, even within 1-km size, the reflectivity excursion above 10 dB is common. We made the linear fit to the relationship of the averaged reflectivity to the nonuniformity strength and found that the nonuniformity increases with increasing averaged reflectivity, in the statistical meaning. The simulation results of the NUBF error indicated that the NUBF error mainly encounters underestimation similar to those from previous studies and cannot be neglected; even in the IFOV whose size is 0.5 km similar to the resolutions of ground-based radars, it can reach up to 50%. We examined the possible correlations between the NUBF error and other parameters such as the reflectivity excursion, the uniform PIA, and the SD and NSD of rain rate, etc., and found that the relative PIA error and the SD of rain rate has a power-law relationship with quite good correlation, which might be used in the rain retrieval algorithm to partially correct this NUBF error. We compared the NUBF errors computed from the 125-m range resolution radar data with those from the simulated 1-km-resolution radar data and found that the difference between them cannot be neglected for the IFOV of 4-km size. This error difference was shown to become more important for the IFOV of a smaller size below 3 km. Because the SRT-based PIA NUBF error is significant for small IFOV (e.g., below 1 km) and the difference between using the high-resolution data and the low-resolution data is also significant for small IFOV, it is very important to use the high-resolution radar data in simulating the NUBF error of spaceborne radar with higher resolutions (e.g., below 3 km) as expected for the next-generation spaceborne radar. The results presented here will provide valuable references for the system design and the rain retrieval algorithm development of the next-generation spaceborne radar.

Acknowledgments. We wish to thank the two anonymous reviewers for their comments and suggestions, which are valuable for improving this paper. This work was supported by the National Natural Science Foundation of China under Contract 40075006, the National High Technology Research and Development Program of China under Contract 2001AA633060, the Department of Science and Technology of China under Projects 2001CCA02200 and 2001CB309402, and the innovation foundation of the Institute of Atmospheric Physics.

REFERENCES

Amayenc, P., M. Marzoug, and J. Testud, 1993: Analysis of cross-beam resolution effects in rainfall rate profile retrieval from a spaceborne radar. *IEEE Trans. Geosci. Remote Sens.,* **GE-31,** 417–425.

——, J. P. Diguet, M. Marzoug, and T. Tani, 1996: A class of single- and dual-frequency algorithms for rain rate profiling from a spaceborne radar. Part II: Tests from airborne radar measurements. *J. Atmos. Oceanic Technol.,* **13,** 142–164.

Durden, S. L., Z. S. Haddad, A. Kitiyakara, and F. K. Li, 1998: Effects of nonuniform beam filling on rainfall retrieval for the TRMM precipitation radar. *J. Atmos. Oceanic Technol.,* **15,** 635–646.

Hitschfeld, W., and J. Bordan, 1954: Errors inherent in the radar measurement of rainfall at attenuating wavelengths. *J. Meteor.,* **11,** 58–67.

Iguchi, T., and R. Meneghini, 1994: Intercomparison of single-frequency methods for retrieving a vertical rain profile from airborne or spaceborne radar data. *J. Atmos. Oceanic Technol.,* **11,** 1507–1516.

——, T. Kozu, R. Meneghini, J. Awaka, and K. Okamoto, 2000: Rain-profiling algorithm for the TRMM precipitation radar. *J. Appl. Meteor.,* **39,** 2038–2052.

Kozu, T., and T. Iguchi, 1999: Nonuniform beamfilling correction for spaceborne radar rainfall measurement: Implications from TOGA COARE radar data analysis. *J. Atmos. Oceanic Technol.,* **16,** 1722–1735.

Marecal, V., T. Tani, P. Amayenc, C. Klapisz, E. Obligis, and N. Viltard, 1997: Rain relations inferred from microphysical data in TOGA COARE and their use to test a rain-profiling method from radar measurements at K_u-band. *J. Appl. Meteor.,* **36,** 1629–1646.

Marshall, J. S., and W. M. Palmer, 1948: The distribution of raindrops with size. *J. Meteor.,* **5,** 165–166.

Meneghini, R., J. Eckerman, and D. Atlas, 1983: Determination of rain rate from a spaceborne radar using measurements of total attenuation. *IEEE Trans. Geosci. Remote Sens.,* **GE-21,** 34–43.

Microwave Remote Sensing Group, 1982: *The Microwave Radiation and Propagation Characteristics of Chinese Clear, Cloudy, and Rainy Atmospheres* (in Chinese). National Defense Industry Press, 161 pp.

Nakamura, K., 1991: Biases of rain retrieval algorithms for spaceborne radar caused by nonuniformity of rain. *J. Atmos. Oceanic Technol.,* **8,** 363–373.

Testud, J., P. Amayenc, and M. Marzoug, 1992: Rainfall-rate retrieval from a spaceborne radar: Comparison between single-frequency, dual-frequency, and dual-beam techniques. *J. Atmos. Oceanic Technol.,* **9,** 599–623.

——, ——, X. Dou, and T. Tani, 1996: Tests of rain profiling algorithms for a spaceborne radar using raincell models and real data precipitation fields. *J. Atmos. Oceanic Technol.,* **13,** 426–453.

Zhang, L., S. Yang, J. Liu, and D. Lu, 1998: A method for retrieving inhomogeneous reflectivity fields within the radar beam (in Chinese). *J. Remote Sens.,* **2,** 81–88.

——, D. Lu, S. Duan, and J. Liu, 2003: Rain spatial nonuniformity and spatial smoothing error of radar rainfall measurement (in Chinese). *Remote Sens. Technol. Appl.,* **18,** 364–373.